Behavior of CaTiO3/nano-CaO as a CO2 reactive adsorbent

ARTICLE *in* INDUSTRIAL & ENGINEERING CHEMISTRY RESEARCH · MARCH 2010

Impact Factor: 2.59 · DOI: 10.1021/ie900900r

2 AUTHORS:

Su Fang Wu
Zhejiang University
38 PUBLICATIONS **390** CITATIONS
SEE PROFILE

Yanqing Zhu
North China University of Water Conservan…
3 PUBLICATIONS **117** CITATIONS
SEE PROFILE

Behavior of $CaTiO_3$/Nano-CaO as a CO_2 Reactive Adsorbent

S. F. Wu* and Y. Q. Zhu

Department of Chemical and Biological Engineering, Zhejiang University, Hangzhou, 310027, China

This study focuses on the preparation of a $CaTiO_3$-coated nano-CaO-based CO_2 adsorbent ($CaTiO_3$/nano-CaO) for the improvement of sorption properties. The $CaTiO_3$-coated nano-CaO adsorbent was prepared by forming $Ti(OH)_4$ from the hydrolysis of titanium alkoxide in a nano-$CaCO_3$ suspended solution. The resulting $Ti(OH)_4$-coated nano-$CaCO_3$ was then heated and calcined. Test results from transmission electron microscopy and scanning electron microscopy with energy dispersive X-ray spectroscopy show that an obvious film of TiO_2 was formed on the surface of nano-$CaCO_3$ after heating. X-ray diffraction analysis also showed that the nano-$CaTiO_3$ layer was formed at 750 °C, a calcination temperature that causes the reaction of TiO_2 with nano-CaO. The cyclic tests of reactive sorption capacity were conducted in a thermogravimetric analyzer under the following conditions: 0.02 MPa CO_2 partial pressure, carbonation temperature of 600 °C, and calcination temperature of 750 °C. Test results showed that $CaTiO_3$ coated onto the nano-CaO caused a significant improvement in the durability of the capacity for reactive sorption. Nano-CaO that had an optimum content of 10 wt % TiO_2 showed significantly stable CO_2 reactive sorption capacity (5.3 mol/kg) after 40 cyclic carbonation−calcination runs compared to the reactive sorption capacity of CaO without TiO_2 coating (3.7 mol/kg).

1. Introduction

A CO_2 adsorption process that employs a solid CaO-based reactive adsorbent plays an important and effective role in the capture of CO_2 for many industrial purposes. For example, CO_2 sorption enhances reformation for hydrogen production,[1−4] promotes CO_2 removal from flue gas,[5,6] and can be utilized for chemical heat pumps[7] and energy storage systems. Although many materials could be potentially used for CO_2 adsorption, CaO has been identified as the most promising candidate[8] because of its stoichiometric reactive sorption capacity, low cost, and the abundance of its natural precursors. However, the natural precursors of CaO-based adsorbents, such as limestone and dolomite that both contain $CaCO_3$, suffer from the rapid decay of CO_2 reactive sorption capacity during multiple carbonation−calcination reaction cycles. Abanades[9] demonstrated a significant decrease in reactive sorption capacity from about 75% during the first carbonation cycle to about 20% in the 14th cycle using 100−800 μm limestone particles.

Aside from its natural precursors, Kuramoto[10] reported a drop in the carbonation conversion of reagent grade $CaCO_3$ and $Ca(OH)_2$ from 50% in the first cycle to 12.2% in the sixth cycle. Florin[11] showed a decline in conversion of CaO adsorbents derived from $CaCO_3$ (Sigma Aldrich, <45 μm) from 69% in the first cycle to only 13% after 50 reaction cycles.

Alvarez[12] found that the decay of the reactive sorption capacity of limestone (400−600 μm) was accompanied by an obvious decrease in the pore volume and surface area. He attributed these to the occlusion of pores and shrinkage of CaO during cycling, which are consequences of sintering. Fierro[13] had proposed a new model to describe the processes of calcination and sintering. He concluded that the main reason for reactive sorption capacity decay is the sintering of CaO during cyclic carbonation−calcination runs. This decay results in subsequent decreases in surface area and porosity and increases in the average CaO particle size.

Several investigations were conducted with the goal of improving the resistance of CaO to sintering. These involved adding MgO,[14] as well as $Ca_{12}Al_{14}O_{33}$, to support the CaO-based CO_2 adsorbent.[15] The author found that nano-$CaCO_3$ had many advantages in comparison to micro-$CaCO_3$. These advantages include higher reactive sorption capacity, fast reaction rate, and a significant improvement in the durability of the adsorbent.[16] The additional investigations have focused on SiO_2-coated nano-$CaCO_3$ as the precursor of nano-CaO-based CO_2 adsorbents. The use of the sol−gel method produced a good reactive sorption capacity of 6.4 mol/kg of the first cyclic run and 4.7 mol/kg of the 20th cyclic run.[17] However, even though the many coating methods provided increased durability during high temperature carbonation and calcination cyclic runs, the overall durability of CaO-based CO_2 adsorbents is still too low for commercial applications.

The hydrolysis method is another technique for preparing metal oxides. Aihara[18] briefly exploited the hydrolysis of $[Ca(OC_2H_5)_2]$ and $[Ti(O\text{-}i\text{-}C_3H_7)_4]$ to form a mixture of CaO and $CaTiO_3$. Guo[19] studied monodispersed silica spheres coated with titania by using $Ti(OC_4H_9)_4$, and Li[20] coated TiO_2 on SiO_2 cores via the hydrolysis of tetrabutyl orthotitanate (TBOT).

This research reports on the preparation of nano-CaO coated with a nanoscale layer of $CaTiO_3$ via hydrolysis and calcination to form a CO_2 adsorbent. Its durability performance and reasons for sintering resistance were investigated.

2. Experimental Section

2.1. Reagents and Instruments. Nano-$CaCO_3$ (>95% purity) with a particle size of 70 nm (Hu Zhou Ling Hua Ltd. China) was used as the CaO-based adsorbent precursor. TiO_2 powder (178 nm, Sinopharm Chemical Reagent Co., Ltd.) and tetrabutyl titanate $Ti(OC_4H_9)_4$ (Sinopharm Chemical Reagent Co., Ltd.) were used as sources of TiO_2.

A thermogravimetric analyzer (TGA, Pyris1, Perkin-Elmer) was used for reactive sorption capacity measurements. The crystalline phases of the components of the adsorbent were determined using an X-ray diffractometer (XRD, D/MAX-RA, Rigaku, Japan). The morphology of the adsorbent was investigated using a transmission electron microscope (TEM, JEM-

* To whom correspondence should be addressed E-mail: wsf@zju.edu.cn. Telephone: +86-571-87953138. Fax: +86-571-87953735.

10.1021/ie900900r
Published on Web 02/11/2010

1230, JEOL, Japan) and scanning electron microscope (SEM, S-4800, HITACHI, Japan). The Ti content was measured by energy-dispersive X-ray analysis (EDX, EX350, HORIBA, Japan). Brunauer−Emmer−Teller (BET) surface area and Barrett−Joyner−Halenda (BJH) desorption average pore diameter analyses were conducted by nitrogen physisorption at liquid N_2 temperatures using a Micromeritics ASAP 2020 apparatus.

2.2. Preparation of TiO_2/Nano-$CaCO_3$. A total of 4.26 g of $Ti(OC_4H_9)_4$ was dissolved in 25 mL of dehydrated ethanol to form a clear solution. A 9 g portion of nano-$CaCO_3$ was dispersed in dehydrated ethanol by ultrasonic methods and then mixed with the clear solution to form a suspension. A 3 g portion of distilled water was added dropwise into the suspension while stirring. Solids were collected by vacuum filtration. The solid product was obtained through drying and heat treatment at 500 °C for 3 h. The first obtained sample is designated as sample A_1.

The mechanism of forming $Ti(OH)_4$ by the hydrolysis of $Ti(OC_4H_9)_4$ proceeds in the following reactions steps (1)−(4):

$$Ti(OC_4H_9)_4 + H_2O \rightarrow Ti(OC_4H_9)_3(OH) + C_4H_9OH \quad (1)$$

$$Ti(OC_4H_9)_3(OH) + H_2O \rightarrow Ti(OC_4H_9)_2(OH)_2 + C_4H_9OH \quad (2)$$

$$Ti(OC_4H_9)_2(OH)_2 + H_2O \rightarrow Ti(OC_4H_9)(OH)_3 + C_4H_9OH \quad (3)$$

$$Ti(OC_4H_9)(OH)_3 + H_2O \rightarrow Ti(OH)_4 + C_4H_9OH \quad (4)$$

The hydrolyzed product was heated to decompose $Ti(OH)_4$ to TiO_2 at a temperature of 500 °C according to the following reactions (5) and (6):

$$H_4TiO_4 \rightarrow H_2TiO_3 + H_2O \quad (5)$$

$$H_2TiO_3 \rightarrow TiO_2 + H_2O \quad (6)$$

A 9 g portion of nano-$CaCO_3$ was dispersed in distilled water by ultrasonic methods, and 1 g of TiO_2 powder was stirred into the suspension. The solids were collected by vacuum filtration and dried. The product obtained in this procedure is designated as sample B_1. Sample B_1 was prepared for the purpose of comparison with sample A_1 in terms of differences in coating and mixing methods.

2.3. Preparation of $CaTiO_3$/Nano-CaO. Samples A_1 and B_1 were calcined at 850 °C for 1 h to form $CaTiO_3$/nano-CaO via the following reactions (7) and (8):

$$CaCO_3 \rightarrow CaO + CO_2 \quad (7)$$

$$CaO + TiO_2 \rightarrow CaTiO_3 \quad (8)$$

Nano-CaO was formed by the decomposition of nano-$CaCO_3$ at 850 °C for 1 h. The resulting CaO was then reacted with TiO_2 to form $CaTiO_3$/nano-CaO. The resulting products after the calcination of samples A_1 and B_1 were designated as samples A_2 and B_2, respectively.

2.4. Test of Reactive Sorption Ratio and Reactive Sorption Capacity. High purity nitrogen gas (N_2) was used as a purge to maintain an accurate TGA balance with a flow rate of 46.37 mL/min. The flow rate of CO_2 was 11.55 mL/min. About 3 mg of the samples were placed in a platinum nacelle. The cyclic CO_2 adsorption tests were conducted under carbonation, with a CO_2 partial pressure of 0.02 MPa in N_2 at 600 °C for less than 10 min, and calcination, with an atmospheric pressure in N_2 at 750 °C for less than 10 min. These steps are similar to those employed by previous researchers.[16,21] The temperature was increased at rates of 15 °C/min for calcination and was decreased at rates of 40 °C/min from calcination temperature to carbonation temperation. The reactive sorption ratio and reactive sorption capacity were calculated according to eqs 1 and 2:

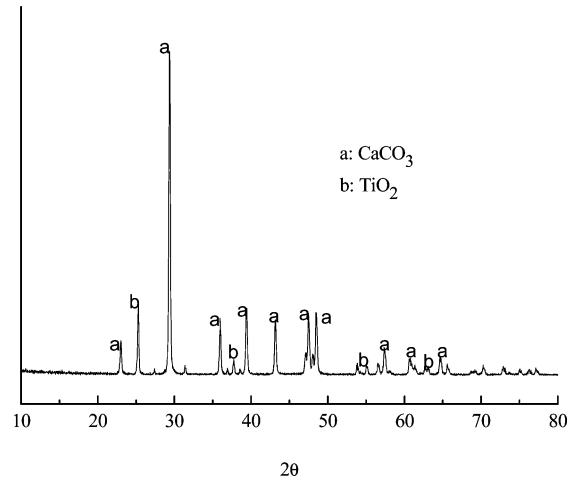

Figure 1. XRD pattern of sample A_1.

$$\text{reactive sorption ratio} = \frac{\text{CO}_2\text{ adsorption mole amount}}{MY/56} \times 100(\%) \quad (1)$$

$$\text{reactive sorption capacity} = \frac{\text{CO}_2\text{ sorption mole amount}}{M} \times 1000(\text{mol kg}^{-1}) \quad (2)$$

where M is the initial mass of the adsorbent and Y is the content of CaO as prepared in the adsorbent.

3. Results and Discussion

3.1. Properties of the TiO_2/Nano-$CaCO_3$. 3.1.1. XRD Pattern. To investigate the coating of nano-TiO_2 on the surface of nano-$CaCO_3$, XRD analysis was performed on sample A_1. TiO_2 was introduced into the $CaCO_3$ structure by hydrolysis (Figure 1).

3.1.2. TEM Images. TEM images of nano-$CaCO_3$ and sample A_1 are shown in Figure 2. Nano-$CaCO_3$ exhibited a cubic crystal, according to Figure 2a. Sample A_1, prepared in a dehydrated ethanol environment, exhibited a flocculelike layer on nano-$CaCO_3$, according to Figure 2b. This layer was composed of a TiO_2 coating. The thickness of the TiO_2 coating was less than 10 nm.

3.1.3. SEM-EDX Images. The SEM images and EDX patterns of the surfaces of nano-$CaCO_3$ and sample A_1 are shown in Figure 3. Compared to that of nano-$CaCO_3$, the particles of sample A_1 had a rough surface layer, where Ti metal was detected by EDX. These confirmed the coating structure. It also confirmed that the hydrolysis product of TiO_2 from titanium alkoxide was indeed formed on the particle surface of sample A_1.

3.1.4. Durability of TiO_2/Nano-$CaCO_3$ Adsorbents. Durability studies of the CO_2 adsorbents at a carbonation temperature of 600 °C and a calcination temperature of 750 °C on nano-$CaCO_3$ and the samples A_1 and B_1 are shown in Figure 4. Nano-$CaCO_3$ recorded a reactive sorption ratio of 84.3% in the

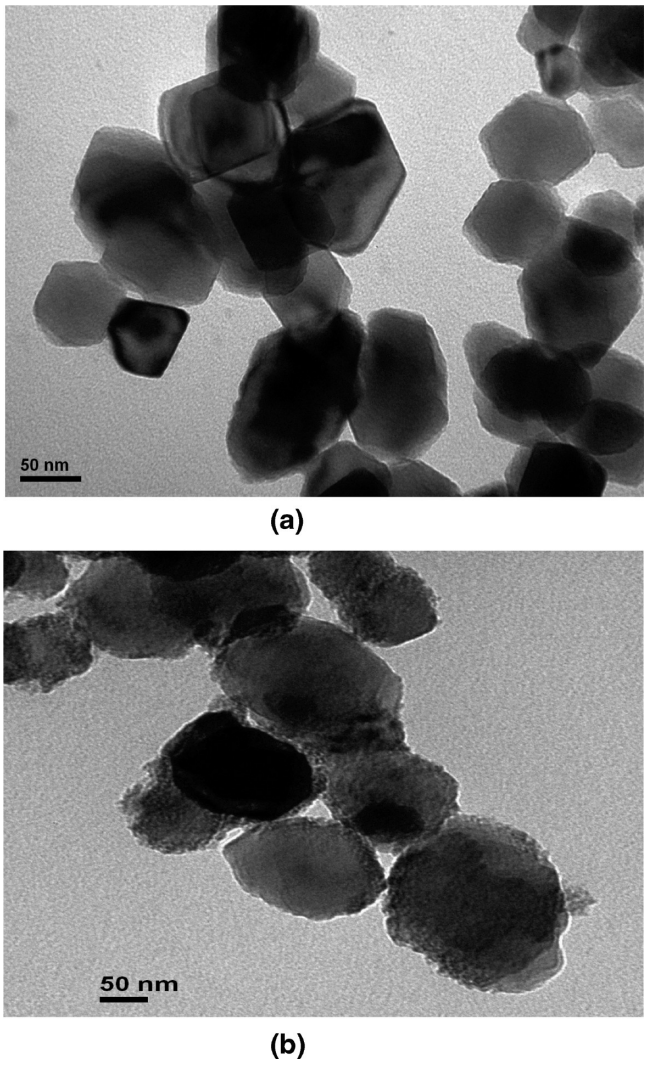

Figure 2. (a) TEM image of nano-$CaCO_3$. (b) TEM image of sample A_1.

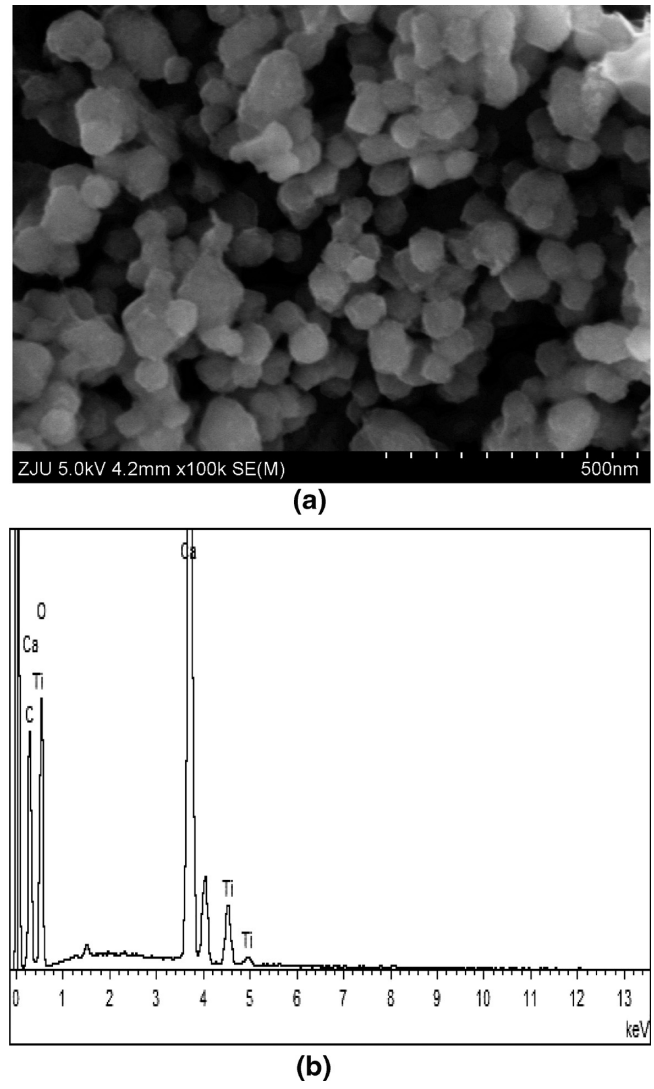

Figure 3. (a) SEM image of sample A_1. (b) EDX result of sample A_1.

first run and the lowest reactive sorption ratio at 37.7% in the tenth run. Sample B_1 had a higher reactive sorption capacity than nano-$CaCO_3$. This indicated that nano-$CaCO_3$ mixed with TiO_2 powder improved the sorption durability of adsorbents. The attenuation trend after 10 runs was also comparable with that of nano-$CaCO_3$. In comparison, sample A_1 showed more stable reactive sorption ratios of 80.6% in the first run and 61.4% in the tenth run. These results indicate that adsorbents prepared via the coating method performed better than those prepared via a simple mixing method.

3.2. Properties of $CaTiO_3$/Nano-CaO Adsorbents. Although TiO_2-coated nano-$CaCO_3$ had a higher reactive sorption ratio, as shown in sample A_1, there was still obvious reactive sorption ratio decay. To improve the durability of sorption, calcination of TiO_2/nano-$CaCO_3$ to form $CaTiO_3$/nano-CaO was performed.

3.2.1. $CaTiO_3$ Identification at Different Calcination Temperatures. To investigate the effects of different calcination temperatures on the formation of $CaTiO_3$ from the reaction between CaO and TiO_2, XRD was performed. It examined the formation of $CaTiO_3$ from sample A_1 at different temperatures. Three temperatures, 750, 800, and 850 °C, were selected for the calcination of sample A_1 for 1 h. Results from this experiment are shown in Figure 5. The figure shows that $CaTiO_3$ already formed at 750 °C but retains only a weak characteristic

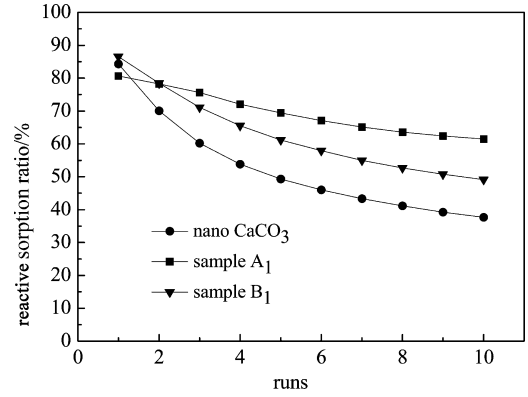

Figure 4. CO_2 reactive sorption ratio for different samples with a number of runs (carbonation at 600 °C in 0.02 MPa CO_2 partial pressure, calcination at 750 °C in N_2).

peak. This temperature is much lower than the $CaTiO_3$ formation temperature, 1200 °C, which was reported in a chemistry handbook.[22] Thus, this supports the formation of a nanoscale layer of $CaTiO_3$ at a lower temperature. At a temperature of 850 °C, the diffraction peaks of $CaTiO_3$ were much stronger, indicating that nano-$CaCO_3$ had completely decomposed to CaO.

3.2.2. Carbonation/Calcination Durability. The reactive sorption capacity of sample A_1, calcined at different tempera-

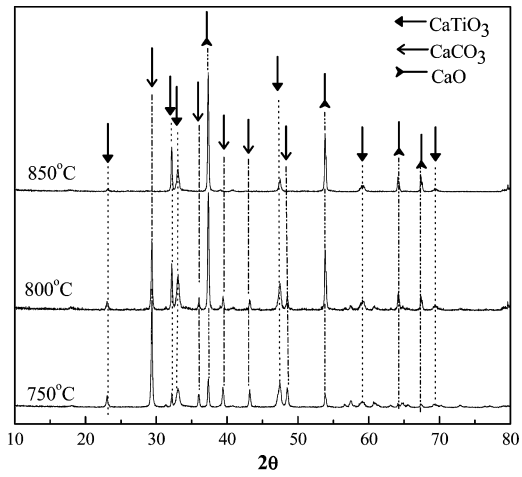

Figure 5. XRD patterns of sample A_1 calcined at different temperatures.

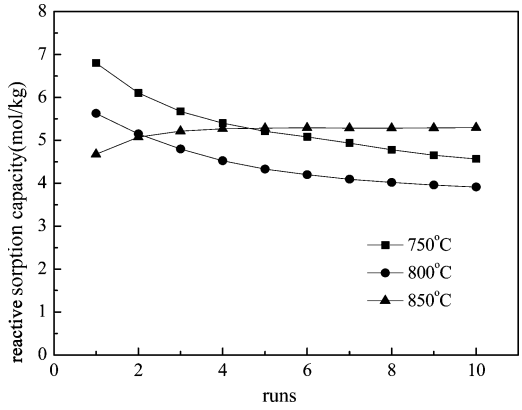

Figure 6. CO_2 reactive sorption capacity for sample A_1 calcined at different temperatures (carbonation at 600 °C in 0.02 MPa CO_2 partial pressure, calcination at 750 °C in N_2).

tures in the range of 750−850 °C, was tested. The sorption capacities after 10 cyclic runs at a sorption temperature of 600 °C and a decomposition temperature of 750 °C are shown in Figure 6. The results show that sample A_1 calcined below 800 °C had a low reactive sorption capacity. In contrast, sample A_1 calcined at 850 °C showed an increase in CO_2 reactive sorption capacity through several initial cycles. This increase in reactive sorption capacity was maintained at 5.3 mol/kg after 10 runs. Manovic[23] disclosed a similar phenomenon called self-reactivation. The results in Figure 6 were consistent with the results shown in Figure 5. Thus, it can be said that sample A_1 calcined below temperatures of 850 °C can form a compound with a stable content of $CaTiO_3$ and increased durability of CO_2 reactive sorption capacity.

The results of the reactive sorption capacity of the nano-CaO, and samples A_2 and B_2 are shown in Figure 7. The reactive sorption capacity of nano-CaO increased in the first several cycles then decreased slightly. In particular, sample A_2 reached a higher reactive sorption capacity than the other samples within three runs, keeping the same reactive sorption capacity after 10 cycles. The reactive sorption capacities of samples A_2 and B_2 were much higher than that of nano-CaO. Sample A_2, which was prepared by the coating method, was more durable than sample B_2 to which TiO_2 was added via a mixing method.

A comparison of the multicycle sorption properties of samples A_1 and A_2 are shown in Figure 8. After 40 cycles, the reactive sorption capacity of TiO_2/nano-$CaCO_3$ was lower than that of $CaTiO_3$/nano-CaO, decaying continuously as the cycles continued. On the other hand, samples of $CaTiO_3$/nano-CaO retained their durability through all experimental runs.

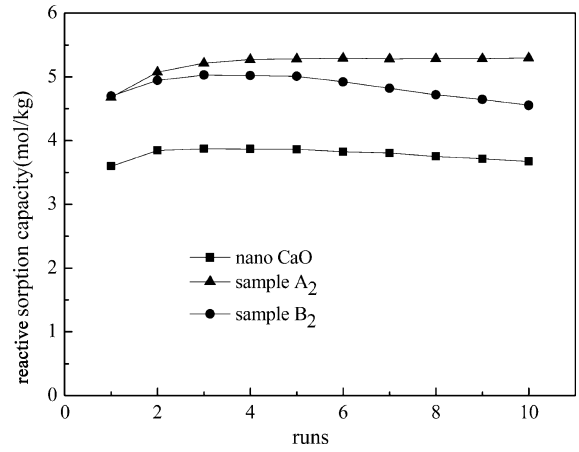

Figure 7. CO_2 reactive sorption capacity for different samples with number of runs (carbonation at 600 °C in 0.02 MPa CO_2 partial pressure, calcination at 750 °C in N_2).

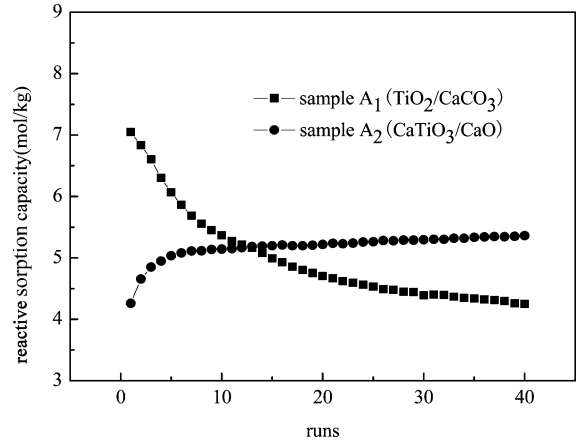

Figure 8. CO_2 reactive sorption capacity for samples A_1 and A_2 with number of runs (carbonation at 600 °C in 0.02 MPa CO_2 partial pressure, calcination at 750 °C in N_2).

Table 1. BET Analytic Results of A_2 before and after 10 Runs[a]

sample	BET surface area (m^2/g)	average pore size (nm)
fresh A_2	6.13	10.15
A_2 after 10 runs	8.29	9.84

[a] Carbonation at 600 °C in 0.02 MPa CO_2 partial pressure, calcination at 750 °C in N_2.

The reactive sorption capacity of sample A_2 in the tenth cycle was 5.3 mol/kg. The reactive sorption capacity of nano-CaO with a TiO_2 coating layer was 1.6 mol/kg higher than that of nano-CaO without the TiO_2 coating. One possible reason for this is that $CaTiO_3$ has a higher melting point (2200 K[18]) and this increases the sintering temperature of the adsorbent. As shown in Figure 8, the reactive sorption capacity of A_2 slightly increased within 10 runs of carbonation and calcination. From the 10th to the 40th run, the reactive sorption capacity was almost stable. The results of BET surface area measurements on A_2 before and after 10 runs are shown in Table 1. The results showed a consistent trend of surface area increase with the increase of reactive sorption capacity.

As shown in Figure 9, SEM morphology analysis showed that $CaTiO_3$/nano-CaO particles have an average size of 80 nm that is maintained after 10 cyclic runs. The $CaTiO_3$ outer layer has high thermal stability and acts as an effective barrier that resists the

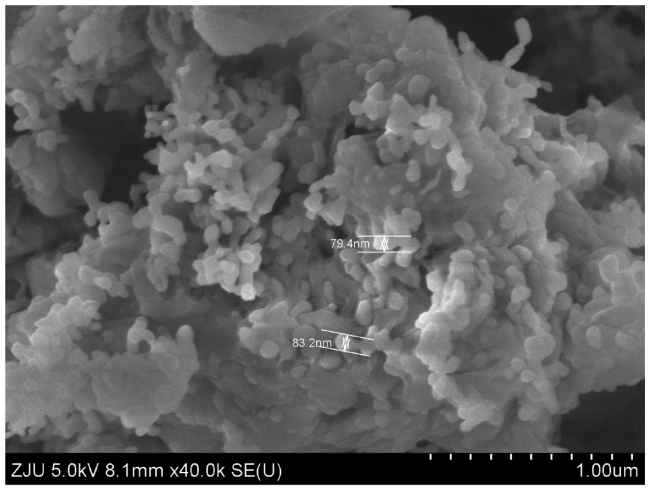

(a)

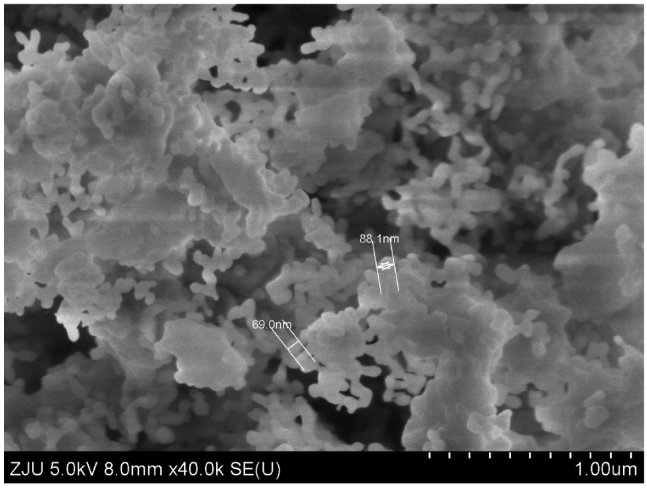

(b)

Figure 9. (a) SEM image of sample A_2 before multiple carbonation−calcination runs. (b) SEM image of sample A_2 after 10 carbonation−calcination runs.

Table 2. Preparation of TiO_2 Coated nano-$CaCO_3$

nano-$CaCO_3$ (g)	$Ti(OC_4H_9)_4$ (g)	H_2O (g)	TiO_2 (wt %)
19	4.26	3	5
11.5			8
9			10
5.67			15
4			20

sintering of CaO, which keeps the structure of the adsorbent more stable even after long-term exposure to elevated temperatures.

3.3. Effects of TiO_2 Content on Cyclic Performances of $CaTiO_3$/Nano-CaO. In order to investigate the effects of TiO_2 content on cyclic performances, five samples with different TiO_2 wt % were prepared by following the synthesis method of sample A_2. Details are listed in Table 2.

TGA test results of reactive sorption capacity are shown in Figure 10. The results showed an optimum TiO_2 content of 10% among compounds containing 5, 8, 10, 15, and 20% TiO_2. It is surmised that when the TiO_2 content was lower than 10 wt %, the TiO_2 amount finally produced from hydrolysis was not enough to cover the surface area of nano-$CaCO_3$. Thus, the resistance to sintering became weak after high temperature calcination. In contrast, when the TiO_2 content was higher than 10 wt %, some active nano-CaO reacted with TiO_2 to form $CaTiO_3$, thus causing the decrease of reactive sorption capacity.

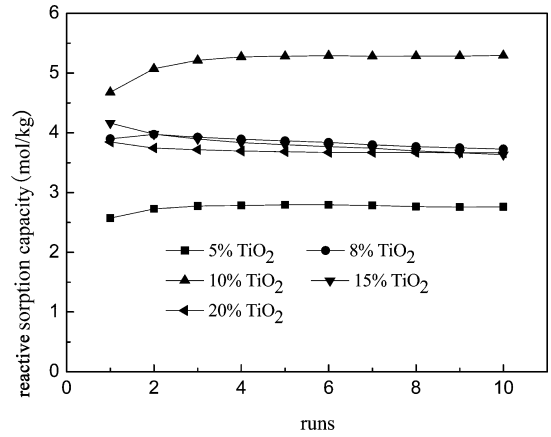

Figure 10. CO_2 reactive sorption capacity for sorbents with different TiO_2 wt % (carbonation at 600 °C in 0.02 MPa CO_2 partial pressure, calcination at 750 °C in N_2).

4. Conclusion

The surface of nano-$CaCO_3$ can be coated with a nano-TiO_2 film via $Ti(OC_4H_9)_4$ hydrolysis and using dehydrated ethanol as a dispersant. A layer of $CaTiO_3$ was formed by calcination at temperatures until 850 °C, thus preventing the nano-CaO particles from coming into contact with each other under high temperatures. Good results were obtained of $CaTiO_3$/nano-CaO adsorbent for the durability of reactive sorption capacity as tested by TGA. Under the same conditions, the 10th cyclic run of the synthesized coated adsorbent had a reactive sorption capacity of 5.3 mol/kg, which was 1.6 mol/kg higher than that of the uncoated nano-$CaCO_3$ adsorbent. Nano-$CaCO_3$ coated with 10 wt % TiO_2 had a maximum reactive sorption capacity during multiple carbonation−calcination cyclic runs.

Acknowledgment

The National Natural Science Foundation of China is thanked for financial support (20676119).

Literature Cited

(1) Han, C.; Harrison, D. P. Simulation Shift Reaction and Carbon Dioxide Separation for the Direct Production of Hydrogen. *Chem. Eng. Sci.* **1994**, *49*, 5875.

(2) Barelli, L.; Bidini, G.; Gallorini, F.; Servili, S. Hydrogen Production through Sorption-Enhanced Steam Methane Reforming and Membrane Technology: A Review. *Energy* **2008**, *33*, 554.

(3) Yi, K. B.; Harrison, D. P. Low-Pressure Sorption-Enhanced Hydrogen Production. *Ind. Eng. Chem. Res.* **2005**, *44*, 1665.

(4) Lee, D. K.; Baek, I. H.; Yoon, W. L. Modeling and Simulation for the Methane Steam Reforming Enhanced by In Situ CO_2 Removal Utilizing the CaO Carbonation for H_2 Production. *Chem. Eng. Sci.* **2004**, *59*, 931.

(5) Gupta, H.; Fan, L. S. Carbonation-Calcination Cycle Using High Reactivity Calcium Oxide for Carbon Dioxide Separation from Flue Gas. *Ind. Eng. Chem. Res.* **2002**, *41*, 4035.

(6) Anthony, E. J. Solid Looping Cycles: A New Technology for Coal Conversion. *Ind. Eng. Chem. Res.* **2008**, *47*, 1747.

(7) Gadalla, M. A.; Olujic, Z.; Jansens, P. J.; Jobson, M.; Smith, R. Reducing CO_2 Emissions and Energy Consumption of Heat-Integrated Distillation Systems. *Environ. Sci. Technol.* **2005**, *39*, 6860.

(8) Feng, B.; An, H.; Tan, E. Screening of CO_2 Adsorbing Materials for Zero Emission Power Generation Systems. *Energy Fuels* **2007**, *21*, 426.

(9) Abanades, J. C.; Alvarez, D. Conversion Limits in the Reaction of CO_2 with Lime. *Energy Fuels* **2003**, *17*, 308.

(10) Kuramoto, K.; Fujimoto, S.; Morita, A.; Shibano, S.; Suzuki, Y.; Hatano, H.; Ying, L. S.; Harada, M.; Takarada, T. Repetitive Carbonation-Calcination Reaction of Ca-based Sorbents for Efficient CO_2 Sorption at Elevated Temperatures and Pressures. *Ind. Eng. Chem. Res.* **2003**, *42*, 975.

(11) Florin, N. H.; Harris, A. T. Enhanced Hydrogen Production from Biomass with In Situ Carbon Dioxide Capture Using Calcium Oxide Sorbents. *Chem. Eng. Sci.* **2008**, *63*, 287.

(12) Alvarez, D.; Abanades, J. C. Pore-Size and Shape Effects on the Recarbonation Performance of Calcium Oxide Submitted to Repeated Calcination/Recarbonation Cycles. *Energy Fuels* **2005**, *19*, 270.

(13) Fierro, V.; Adánez, J.; García-Labiano, F. Effect of Pore Geometry on the Sintering of Ca-Based Sorbents During Calcination at High Temperatures. *Fuel* **2004**, *83*, 1733.

(14) Dobner, S.; Sterns, L.; Graff, R. A.; Squires, A. M. Cyclic Calcination and Recarbonation of Calcined Dolomite. *Ind. Eng. Chem., Process Des. Dev.* **1977**, *16*, 479.

(15) Li, Z. S.; Cai, N. S.; Huang, Y. Y.; Han, H. J. Synthesis, Experimental Studies, and Analysis of a New Calcium-Based Carbon Dioxide Absorbent. *Energy Fuels* **2005**, *19*, 1447.

(16) Wu, S. F.; Li, Q. H.; Kim, J. N.; Yi, K. B. Properties of a Nano CaO/Al_2O_3 CO_2 Sorbent. *Ind. Eng. Chem. Res.* **2008**, *47*, 180.

(17) Wu, R.; Wu, S. F. The Performance of Nano-Calcium Coated with SiO_2 on CO_2 Adsorption and Regeneration. *Chin. J. Chem. Eng.* **2006**, *57*, 1722.

(18) Aihara, M.; Nagai, T.; Matsushita, J.; Negishi, Y.; Ohya, H. Development of Porous Solid Rreactant for Thermal-Energy Storage and Temperature Upgrade Using Carbonation/Decarbonation Reaction. *Appl. Energy* **2001**, *69*, 225.

(19) Guo, X. C.; Dong, P. Multistep Coating of Thick Titania Layers on Monodisperse Silica Nanospheres. *Langmuir* **1999**, *15*, 5535.

(20) Li, Q. Y.; Dong, P. Preparation of Nearly Monodisperse Multiply Coated Submicrospheres with a High Refractive Index. *J. Colloid Interface Sci.* **2003**, *261*, 325.

(21) Wu, S. F.; Beum, T. H.; Yang, J. I.; Kim, J. N. Properties of Ca-Base CO_2 Sorbent Using $Ca(OH)_2$ as Precursor. *Ind. Eng. Chem. Res.* **2007**, *46*, 7896.

(22) Liu, Y. Z. *Manual for Physicochemical Properties of Inorganic Substances and Important Reaction Equations*; Chengdu University of Science and Technology Publisher: Chengdu, 1993.

(23) Manovic, V.; Anthony, E. J. Thermal Activation of CaO-Based Sorbent and Self-Reactivation during CO_2 Capture Looping Cycles. *Environ. Sci. Technol.* **2008**, *42*, 4170.

Received for review June 4, 2009
Revised manuscript received January 21, 2010
Accepted January 21, 2010

IE900900R